Ergonomics, Vol. 48, No. 6, 15 May 2005, 625–641

Taylor & Francis
Taylor & Francis Group

3D foot shape generation from 2D information

AMEERSING LUXIMON†, RAVINDRA S. GOONETILLEKE‡* and MING ZHANG†

†Jockey Club Rehabilitation Engineering Center, Hong Kong Polytechnic University, Hung Hom, Kowloon, Hong Kong
‡Department of Industrial Engineering and Engineering Management, Hong Kong University of Science and Technology, Clear Water Bay, Kowloon, Hong Kong

Two methods to generate an individual 3D foot shape from 2D information are proposed. A standard foot shape was first generated and then scaled based on known 2D information. In the first method, the foot outline and the foot height were used, and in the second, the foot outline and the foot profile were used. The models were developed using 40 participants and then validated using a different set of 40 participants. Results show that each individual foot shape can be predicted within a mean absolute error of 1.36 mm for the left foot and 1.37 mm for the right foot using the first method, and within a mean absolute error of 1.02 mm for the left foot and 1.02 mm for the right foot using the second method. The second method shows somewhat improved accuracy even though it requires two images. Both the methods are relatively cheaper than using a scanner to determine the 3D foot shape for custom footwear design.

Keywords: Mass customization, Footwear, Foot outline, Fitting, Foot shape modeling

1. Introduction

Three-dimensional image construction from 2D images is essential in many applications ranging from geology (Liu 2003) to robotics (Gavrila and Groen 1992). In geology, methods such as photogrammetry, Synthetic Aperture Radar Interferometry (InSAR), radar altimetry and Light Detection And Ranging (LIDAR) technology (Liu 2003) are used to capture elevation data. A good discussion of the advantages and disadvantages of the different techniques is provided by Toutin and Gray (2000). Since these techniques are of relatively high cost, more cost effective techniques have been developed. Liu (2003) used the shading information of single image data to derive the surface topography using a technique called shape-from-shading. Various shape-from-shading techniques have been proposed (Bingham and Rees 1999, Wildey 1986). The shape-from-shading

*Corresponding author. Email: ravindra@ust.hk

Ergonomics
ISSN 0014-0139 print/ISSN 1366-5847 online
http://www.tandf.co.uk/journals
DOI: 10.1080/0014013050070970

technique has recently been used to estimate facial pose (Choi et al. 2002). Such techniques are generally used to determine elevation or create surface maps and thus different methods have to be used if the complete 3D shape is required.

In robotics and telerobotics, video images are used to determine object shapes. Gavrila and Groen (1992) provided a 'geometric hashing' technique to improve robot vision, which involves storing the differing 2D views of the 3D object in a table (hash table). Then a filtering method is used to select the object from the infinite possibilities in the hash table. The algorithm has been tested using 3D text shapes of letters, M, A, R, L, E and N but the approach has its weaknesses with complex models and in noisy environments. Furthermore, the hashing method requires large storage capacity, thereby limiting the number of models in a database. Triboulet et al. (1996) proposed a method to locate objects which were polyhedral and cylindrical. Their method used an infra-red range finder to find the distance between the object and the robot and a person provided 2D data into the system. Similar techniques have been used in computer-aided design to generate 3D solid models from orthogonal views (Tam and Atkinson 2003). These applications all rely on recognition methods to generate simple geometric models. This paper is an attempt to generate the complex 3D foot shape from a "standard" foot shape and 2D information with respect to the outline and height. The first method requires the foot outline and foot height, while the second method requires foot outline and foot profile.

Three dimensional laser scanners are becoming popular for 3D shape generation. These systems are relatively expensive and hence cheaper alternatives will help manufacturers to collect sufficient data to deliver consumer goods such as footwear economically. Luximon and Goonetilleke (2004) discussed a foot shape prediction model using simple anthropometric measures. That model was developed using forty Hong Kong Chinese males and then validated using a different group of twenty-five Hong Kong Chinese males. The model was based on the parameterization of a "standard" foot using the four parameters of foot length, foot width, foot height, and foot curvature. The predicted shape had a mean accuracy of 2.1 mm for the left foot and 2.4 mm for the right foot. In the present paper, an improved method is proposed based on an after-thought when trying to obtain the four parameters required for the Luximon and Goonetilleke (2004) model. Even though those four parameters can be measured using a simple scale and protractor, webcams, digital cameras or even 35mm cameras can be used to first capture foot images that can then be "digitized" to give out the necessary dimensions (Hung et al. 2004). However, this process of digitizing images "throws away" valuable information in relation to shape. This paper is based on the rationale that the captured images can be more effectively used for foot shape prediction rather than just a few dimensions obtained from the captured images. More specifically, the top or bottom view of the foot can be processed to give the foot outline (figure 1a) while a side-view gives the foot profile or the foot height along the length of the foot (figure 1b).

2. Methodology

2.1 *Participants*

Eighty Hong Kong Chinese males, who were students and staff from the Hong Kong University of Science and Technology, participated in this study. A standard foot was generated using the "mean" of forty participants as reported in the Luximon and

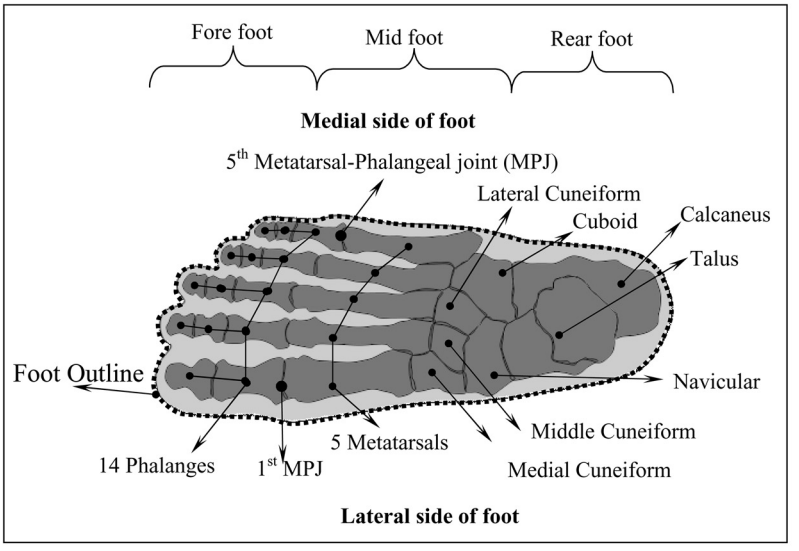

(a) Foot outline

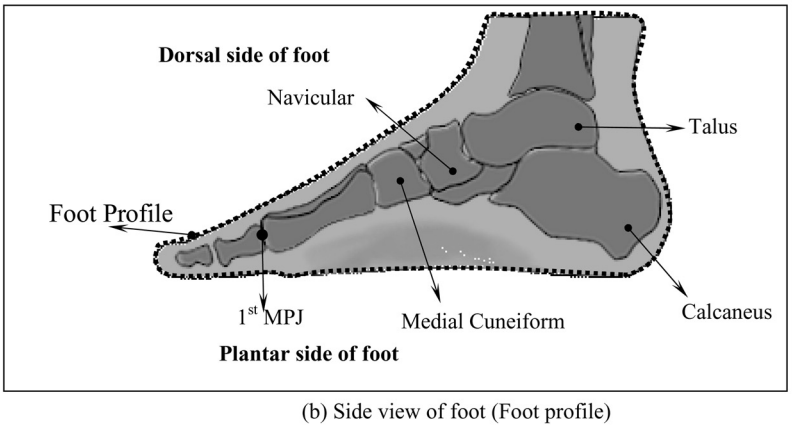

(b) Side view of foot (Foot profile)

Figure 1. Outline and profile of foot.

Goonetilleke (2004) study while the data of the other forty participants were used to validate the two proposed models. None of the participants had any foot illness or foot abnormalities. Each participant was paid HK$75 (~USD 10) for their time.

2.2 *Procedure*

Each participant signed a consent form, and thereafter their age, height and weight were recorded. Their feet were washed and disinfected using an antiseptic germicide in a foot bubble roller massager. The water temperature was maintained at $25 \pm 1^{\circ}C$ using a DigiSense Thermistor. After drying their feet, the foot length, arch length and foot width were measured using the Brannock device (Brannock 2004) while the participant stood on both feet. Each participant's feet were scanned using a Yeti 3D laser scanner (Vorum Research Corporation 1998). The participant stood with one foot on the glass platform

inside the scanner, while the other foot was on a weighing scale to ensure that the weight on each foot was half body weight. The complete procedure is described in detail in Luximon and Goonetilleke (2004). The 3-D point cloud data obtained from the scanner was processed and analysed using MATLAB version 5 with Spline Toolbox.

2.3 *Prediction Model*

In order to generate the standard shape, each foot was first aligned along the heel center line, which was defined as the line separating the heel into equal halves in the heel region (corresponding to 20% of the foot length) (Luximon and Goonetilleke 2004). The aligned foot was then sectioned at each 1% foot length so that there were 99 sections. The points of each section were then sampled at a fixed angular interval of 1° so that there were 360 points per section. Hence each foot had points with coordinates $p_{ij} = (x_{ij}, y_{ij}, z_{ij})$, where $i = 1,\ldots,99$; $j = 1,\ldots,360$. The width, dorsal height and height (dorsal height minus plantar height) of each section were w_i, h_i, and H_i respectively. When the corresponding foot section is touching the XZ-plane, the dorsal foot height (h_i) is equal to height (H_i) as shown in Figure 2. Averaging the points of different subjects created the standard foot. The standard foot had points $\bar{p}_{ij} = (\bar{x}_{ij}, \bar{y}_{ij}, \bar{z}_{ij})$ with width = $\bar{w}_i$, dorsal height = $\bar{h}_i$, and height = $\bar{H}_i$ (where $i = 1,..,99$; $j = 1,\ldots,360$) as shown in figure 2. Recursive regression equations were developed for each parameter between adjacent pairs of sections. Since there were 99 sections, there were 98 regression equations for height. If the section height of a 'seed' section is known, the section heights of the remaining sections can be predicted recursively using the 98 regression equations. The location of the 'seed' section can

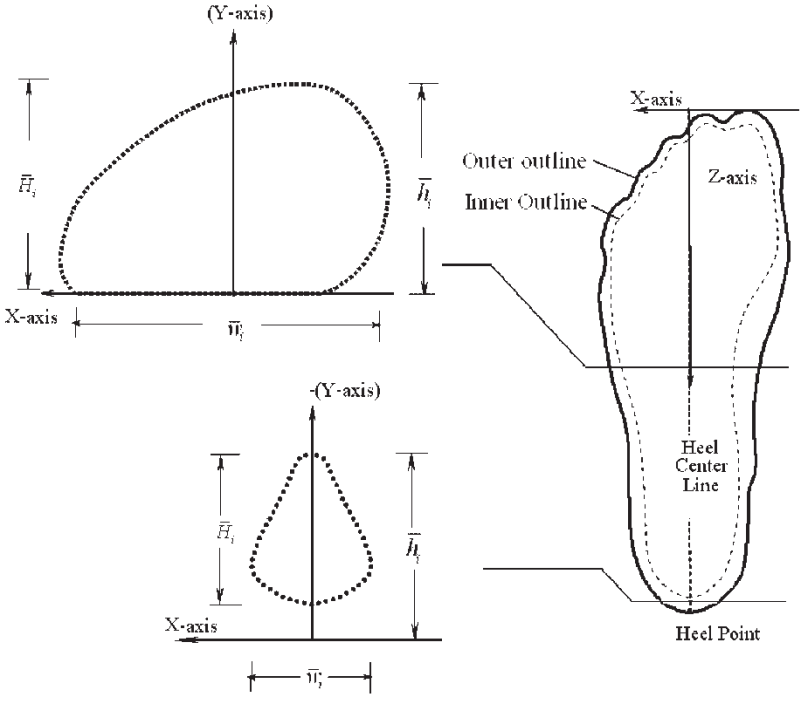

Figure 2. Axis system of standard foot.

influence the overall prediction accuracy, and so an optimum 'seed' section (μ) was calculated such that the prediction error for that parameter was minimized. In this study, the standard foot shape (figure 2) was developed using the same forty participants as the Luximon and Goonetilleke (2004) study.

Method I: The first method used the 2D foot outline and dorsal foot height (h_μ) at the optimum seed section of the participant whose 3D foot shape was to be determined. The recursive regression equations were used to determine the dorsal foot height of the sections (i = 1,.., $\mu - 1$, $\mu + 1$,...,99) using the dorsal foot height (h_μ). The predicted dorsal foot heights, $\hat{h}_{i\mu}$ (i = 1,..,99; $\hat{h}_{\mu\mu} = h_\mu$) were then used for scaling the standard foot. The width of each section of the standard foot was adjusted to match the foot outline (figure 3a). Then, the standard foot section heights were scaled using the predicted height ($\hat{h}_{i\mu}$) as shown in figure 3a. The height-scaling factor was ($\hat{h}_{i\mu}/\bar{h}_i$), while the width-scaling factor was ($w_i/\bar{w}_i$) for each section. The scaling for each individual section was different. Finally, the length of the outline was used to scale the z-coordinate. The predicted foot using foot outline and dorsal foot height at optimum seed (method I) had points ${}_I\hat{p}_{ij} = ({}_I\hat{x}_{ij}, {}_I\hat{y}_{ij}, {}_I\hat{z}_{ij})$. Figure 3a shows the shape changes of a section near the heel as it undergoes the various transformations. The sequence of the transformations is shown in parenthesis.

Method II: The inputs to the second method were the foot outline and foot profile. The foot shape was created by modifying the standard foot using the measured height and width obtained from the foot outline and profile respectively. The width scaling and height scaling for the sections were ($w_i/\bar{w}_i$) and ($H_i/\bar{H}_i$) respectively. The parentheses in figure 3b indicates the transformation sequence for a section near the heel. The predicted foot shape was generated after length scaling of the standard foot using the foot outline. The predicted foot using foot outline and foot profile (method II) had points ${}_{II}\hat{p}_{ij} = ({}_{II}\hat{x}_{ij}, {}_{II}\hat{y}_{ij}, {}_{II}\hat{z}_{ij})$.

The models were validated using a different set of 40 participants (25 of whom were the same as in the Luximon and Goonetilleke (2004) study). After the shape prediction and alignment, using the two methods, the prediction error was calculated using the dimensional difference between the predicted shape and the actual foot shape (Luximon and Goonetilleke 2004).

3. Results

Table 1 shows the descriptive statistics of the two groups of participants. The optimum seed to predict the right foot height was at 52% of foot length from toe ($\mu = 52$), and the optimum seed to predict the left foot height was at 55% of foot length from toe ($\mu = 55$) (Luximon and Goonetilleke 2004). After the foot shapes were generated, the error between the predicted foot shape and the actual foot shape was computed for each of the two methods. The error was defined as the Euclidean distance from points on the actual foot shape to the closest point on the predicted shape (Luximon and Goonetilleke 2004; Luximon et al. 2003). The mean, maximum and minimum error of the 40 subjects for left and right feet were calculated and are shown in table 2 (for method I) and table 3 (for method II). For method I, the mean error was 1.37 mm (SD. = 0.30 mm) for the right foot and 1.36 (SD. = 0.39) for the left foot. For method II, the average error was 1.02 mm (SD. = 0.21 mm) for the right foot and 1.02 (SD. = 0.18) for the left foot. An example of the error (= actual - predicted) plot for each of the two prediction methods is

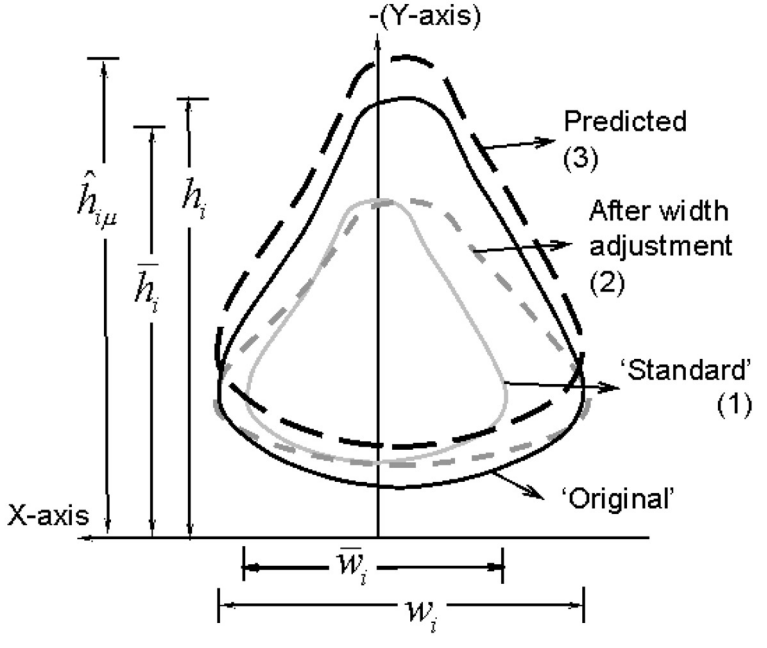

(a)

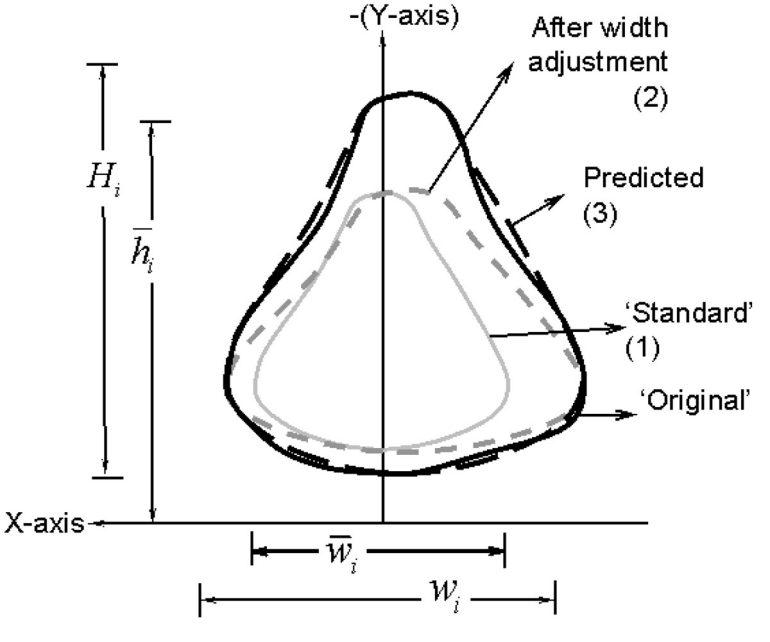

(b)

Figure 3. Generation of predicted sections from the standard section using (a) method I and (b) method II.

Table 1. Descriptive statistics of participants. Conversion from Brannock units to centimetres is based on Goonetilleke et al. (1997).

	Participants for model generation (n = 40)				Participants for model validation (n = 40)			
	Mean	Max.	Min.	SD.	Mean	Max.	Min.	SD.
Age	22.0	36	19	3.36	21.3	41	19	3.39
Weight (kg)	62.75	89.8	47.2	8.52	64.69	88.3	47.35	8.05
Height (cm)	171.3	183.4	160.1	5.55	173.3	186.1	161.3	6.19
Right foot								
Foot Length (cm)	25.55	28.3	23.5	1.11	25.92	28.3	23.6	1.10
Foot Width (cm)	9.91	11.2	9.0	0.50	9.96	11.2	9.0	0.45
Arch Length (cm)	18.70	17.1	21.8	0.96	18.82	17.1	20.4	0.84
Left foot								
Foot Length (cm)	25.54	28.3	23.1	1.11	25.87	27.8	23.8	1.13
Foot Width (cm)	10.00	11.6	9.0	0.51	10.01	11.2	9.2	0.47
Arch Length (cm)	18.47	16.5	21.8	1.01	18.61	17.1	20.4	0.85

Table 2. Mean, minimum and maximum error (mm) between the 'actual' feet and the predicted feet using prediction method I (foot outline and height) for 40 participants

	Left				Right			
Participant	Mean	SD	Min.	Max.	Mean	SD	Min.	Max.
1	2.01	2.28	− 6.23	7.99	1.46	1.78	− 6.07	5.30
2	1.40	1.80	− 6.78	4.25	1.36	1.75	− 7.04	5.34
3	1.32	1.98	− 10.14	9.95	1.25	1.63	− 8.07	6.50
4	1.01	1.22	− 5.17	4.34	1.33	1.65	− 7.33	5.05
5	1.61	1.80	− 4.73	6.39	1.66	2.03	− 8.21	5.83
6	1.33	1.67	− 8.62	6.74	1.26	1.33	− 6.77	5.41
7	1.23	1.55	− 4.79	6.36	0.95	1.22	− 4.02	5.94
8	1.39	1.24	− 4.58	4.23	1.58	1.57	− 6.14	5.45
9	2.82	3.64	− 13.10	8.90	2.21	2.84	− 9.07	7.60
10	1.29	1.60	− 6.49	4.39	1.43	1.83	− 7.69	5.80
11	1.31	1.22	− 4.45	5.22	1.50	1.46	− 4.66	5.94
12	1.03	1.33	− 4.23	6.67	1.32	1.64	− 4.03	8.59
13	1.41	1.47	− 4.22	5.22	1.11	1.23	− 4.07	5.55
14	1.47	1.74	− 5.33	8.22	1.51	1.79	− 5.99	6.89
15	1.07	1.40	− 7.48	6.29	1.00	1.32	− 6.08	5.14
16	1.63	2.35	− 8.88	8.40	1.39	1.85	− 5.61	6.37
17	1.10	1.39	− 4.98	5.61	1.61	2.13	− 8.11	7.00
18	1.71	1.96	− 5.73	6.61	1.51	1.74	− 6.49	6.77
19	1.39	1.59	− 5.60	5.60	1.69	2.24	− 4.32	8.49
20	1.11	1.29	− 3.47	6.05	1.14	1.32	− 3.33	5.26
21	1.26	1.72	− 7.06	5.75	1.51	2.04	− 7.62	8.03
22	0.81	0.95	− 2.85	3.80	0.99	1.23	− 4.33	3.81
23	2.16	2.83	− 8.65	9.59	1.95	2.45	− 6.92	8.98
24	0.99	1.18	− 4.01	5.13	1.24	1.53	− 5.56	6.47
25	1.39	2.08	− 7.02	10.99	1.36	2.07	− 7.73	11.27
26	1.56	2.20	− 5.61	9.77	2.02	2.38	− 6.03	8.12
27	1.36	1.75	− 4.19	7.70	1.73	2.04	− 6.27	7.72
28	1.14	1.25	− 3.57	4.99	1.13	1.18	− 2.87	5.09
29	1.14	1.43	− 5.87	4.48	1.09	1.32	− 5.19	4.10
30	1.43	1.73	− 6.10	5.23	1.24	1.51	− 6.59	5.04
31	1.62	2.21	− 8.07	9.75	1.38	1.77	− 7.45	7.03
32	0.90	1.16	− 3.74	6.24	1.50	1.91	− 5.62	7.16
33	1.08	1.40	− 3.34	5.26	1.04	1.06	− 5.64	4.31
34	1.16	1.40	− 4.29	4.77	0.97	1.27	− 4.64	6.84
35	1.43	1.72	− 5.83	6.05	1.53	1.95	− 5.39	6.88
36	1.29	1.51	− 5.61	4.50	1.24	1.31	− 5.29	4.70
37	2.16	2.81	− 10.03	11.53	1.60	1.99	− 6.61	7.63
38	1.15	1.58	− 5.24	6.20	1.03	1.25	− 4.47	4.61
39	0.84	1.04	− 3.87	4.94	1.11	1.28	− 4.50	4.74
40	0.94	0.99	− 2.54	4.90	0.96	1.12	− 4.93	4.40
Mean	1.36	1.69	− 5.81	6.47	1.37	1.67	− 5.92	6.28
SD	0.39	0.55	2.22	2.03	0.30	0.41	1.47	1.56

shown in figure 4 using gray-scale-codes. Only the right foot plot is shown, as the plot for the left foot was similar. A 'flattened' or 2D representation (2D-Rep) of the error is also shown in figure 4. The 2D-representation shows the 99 sections*360 points (at 1° degrees interval) on the surface of the foot. The different locations such as medial, dorsal, lateral and plantar sides as well as the fore-foot, mid-foot and rear-foot can easily be identified in

Table 3. Mean, standard deviation, minimum and maximum error (mm) between the 'actual' feet and the predicted feet using prediction method II (foot outline and foot profile) for 40 participants

	Left				Right			
Participant	Mean	SD	Min.	Max.	Mean	SD	Min.	Max.
1	1.08	1.40	− 5.73	6.28	0.96	1.34	− 6.05	5.14
2	0.96	1.42	− 6.69	2.64	0.85	1.24	− 7.02	2.93
3	1.23	1.91	− 9.91	10.09	1.06	1.40	− 7.30	5.93
4	0.72	0.92	− 5.15	3.30	1.01	1.43	− 7.31	4.42
5	1.13	1.37	− 4.85	6.50	1.09	1.40	− 8.20	6.00
6	0.87	1.21	− 8.63	3.81	0.88	1.07	− 6.74	4.59
7	0.91	1.23	− 3.00	5.90	0.84	1.13	− 3.25	5.94
8	0.87	1.01	− 4.58	4.37	1.05	1.27	− 6.13	5.41
9	1.76	2.70	− 13.17	6.07	1.35	1.99	− 8.99	4.21
10	1.02	1.33	− 6.48	4.00	1.12	1.50	− 7.63	5.79
11	0.98	1.11	− 4.36	5.59	1.15	1.25	− 4.78	4.92
12	0.91	1.23	− 4.30	6.74	0.99	1.39	− 3.93	8.52
13	0.88	1.08	− 3.98	4.23	0.88	1.11	− 4.07	5.54
14	1.08	1.44	− 5.39	7.08	1.11	1.49	− 6.27	8.28
15	0.90	1.22	− 6.54	4.18	0.87	1.16	− 5.52	4.62
16	1.19	1.68	− 7.86	7.87	0.91	1.20	− 4.59	5.98
17	0.93	1.23	− 5.04	5.88	1.19	1.71	− 7.18	7.74
18	0.98	1.27	− 4.65	5.58	1.23	1.58	− 6.48	6.77
19	1.16	1.53	− 5.61	5.62	1.28	1.76	− 4.31	9.31
20	0.91	1.17	− 3.68	6.05	0.84	1.12	− 3.42	5.19
21	1.13	1.51	− 6.74	5.74	1.31	1.82	− 7.41	7.98
22	0.74	0.87	− 2.89	3.45	0.82	1.05	− 4.31	4.84
23	1.44	2.13	− 8.72	7.15	1.33	1.86	− 7.02	7.05
24	0.83	1.07	− 4.64	4.06	0.92	1.22	− 5.57	5.97
25	1.36	2.14	− 7.03	10.99	1.25	2.08	− 7.73	11.31
26	1.25	1.96	− 5.68	9.74	1.53	2.27	− 5.51	10.13
27	1.24	1.68	− 4.25	7.67	1.17	1.51	− 6.80	5.55
28	0.76	0.90	− 2.94	3.30	0.83	1.07	− 3.15	5.05
29	0.93	1.24	− 5.83	4.50	0.91	1.16	− 5.20	4.96
30	1.00	1.35	− 6.01	5.23	0.96	1.29	− 6.47	4.78
31	1.16	1.70	− 7.23	10.57	1.07	1.53	− 7.16	8.87
32	0.75	1.01	− 4.29	6.29	0.87	1.20	− 3.96	7.51
33	0.88	1.22	− 3.03	6.95	0.78	0.99	− 5.63	4.32
34	0.93	1.17	− 4.28	4.29	0.88	1.19	− 4.61	6.88
35	0.95	1.24	− 5.86	6.02	1.03	1.35	− 3.79	7.38
36	0.95	1.27	− 5.64	3.71	0.82	1.04	− 5.35	4.69
37	1.29	1.86	− 10.04	7.89	1.00	1.32	− 6.86	5.80
38	1.11	1.54	− 5.23	6.20	0.92	1.17	− 4.49	4.62
39	0.79	0.96	− 3.01	5.22	0.87	1.12	− 4.51	4.57
40	0.82	0.96	− 2.89	4.89	0.80	1.04	− 4.91	3.73
Mean	1.02	1.38	− 5.65	5.89	1.02	1.37	− 5.74	6.08
SD	0.21	0.39	2.21	2.01	0.18	0.31	1.50	1.83

the 2D-representation plots. From the 2D plot, it can be seen that there are high positive errors around the toe region (1st and 2nd toe), medial side of mid-foot (around arch region) and at the medial talus region, while there were high negative errors at the lateral talus region when method I prediction model was used. Similarly, there were high positive

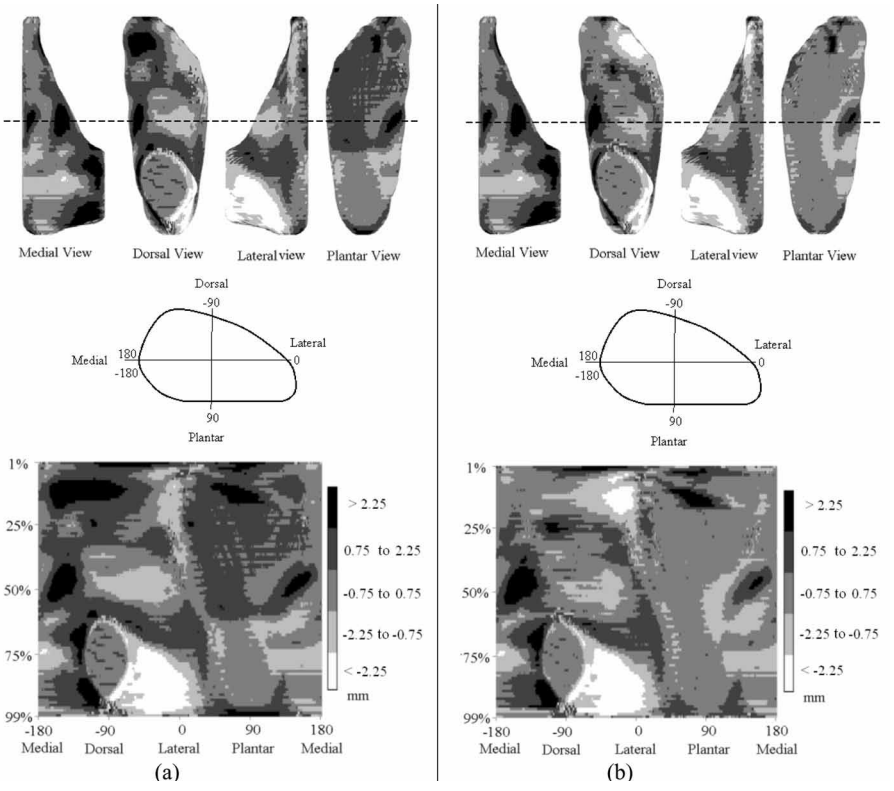

Figure 4. Right foot of one participant (number 40) with gray-scale-coded error with (a) method I and (b) method II.

errors at the medial side of mid-foot (arch region) and at the medial talus region, while there are high negative errors at the lateral talus region and at the dorsal side of the 3rd to 5th toe when method II prediction model were used. The shades of gray are different in the different regions and hence statistical analyses were performed in order to have a better understanding of the differences between methods I, II and the previous Luximon and Goonetilleke (2004) method (denoted as L&G).

The same 25 subjects used to validate the prediction model in the Luximon and Goonetilleke (2004) study were used here. Figures 5a, 5b, and 5c show the mean and the standard deviation (n = 25) for the right foot shape when using the L&G method, the proposed method I, and method II respectively. A quick comparison shows that the errors at most locations on the foot surface are higher with the L&G method. The error seems higher (error $\approx$ 3mm) on the lateral side of foot and at the rear foot. Also, with the L&G method, it seems that there is a higher variation (dark color = 5mm) on both medial and lateral sides of the rear foot. In addition, method I seems to show a higher error on both dorsal and plantar side of the foot when compared to method II (figures 5b and 5c). These visual differences among the three methods were tested using statistical analyses on the 99 $\times$ 360 = 35640 points of both feet of the 25 subjects. A statistical analysis program was written in MATLAB for this purpose. The results of the pairwise T-test comparisons 35640 $\times$ 3 are shown in figures 6a, 6b, and 6c. The figures 7a, 7b, and 7c show the differences in mean. The results for the left foot were similar. L&G had

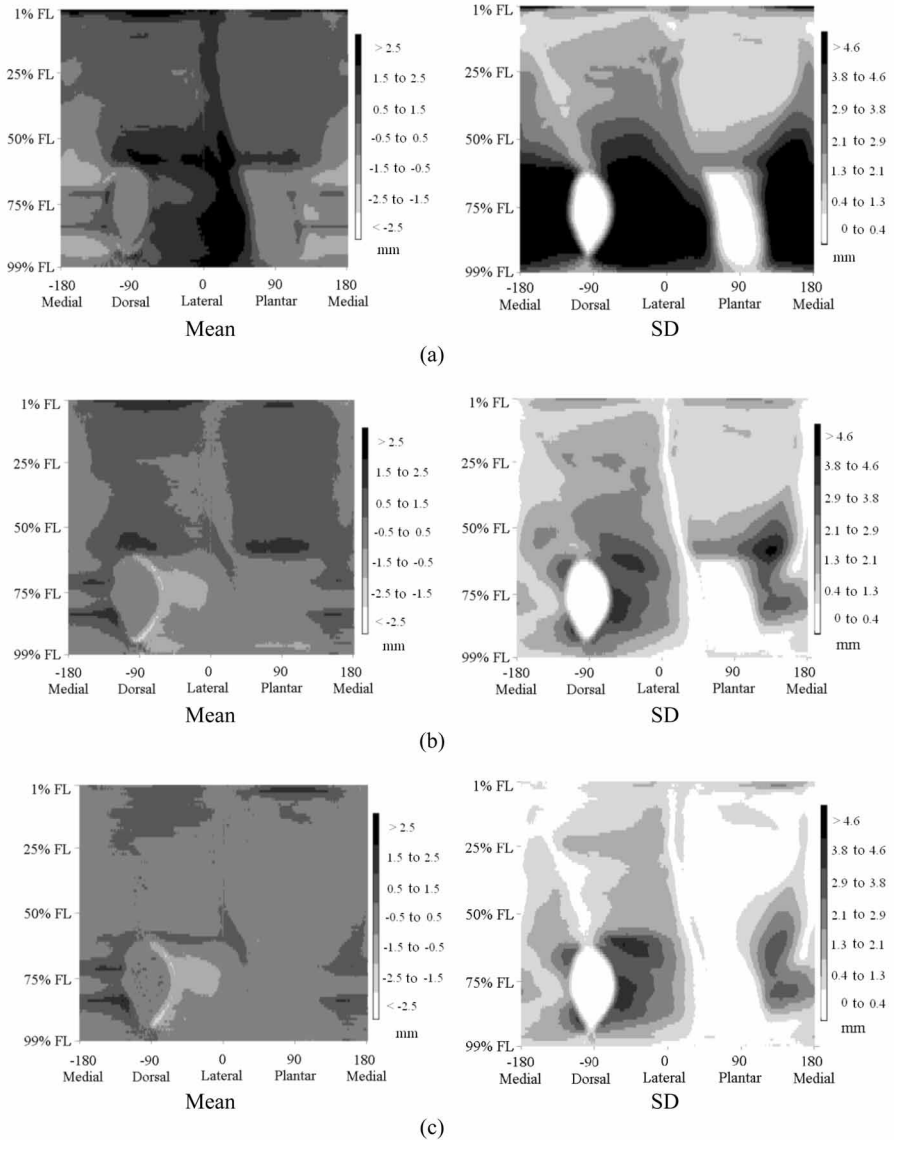

Figure 5. Gray-scale-coded mean prediction error (mm) compared to actual foot and standard deviation (n = 25) at each point (360 × 99) on the right foot surface when using (a) Method L&G, (b) Method I, (c) Method II (FL denotes foot length).

statistically higher mean absolute error at the rear foot and medial side of mid foot (dorsal cuneiform or arch region) when compared to method I. At the rear foot, L&G had higher errors around the malleolus, the heel (back of foot) and the plantar side of the navicular regions. Method II had statistically lesser mean absolute error at the rear foot (both dorsal and plantar side), and dorsal side of forefoot {metatarsal region and metatarsal-phalangeal joint (MPJ) region} and plantar toe regions when compared to L&G. The difference in absolute error was least ($\approx -$ 1mm) around the lateral and

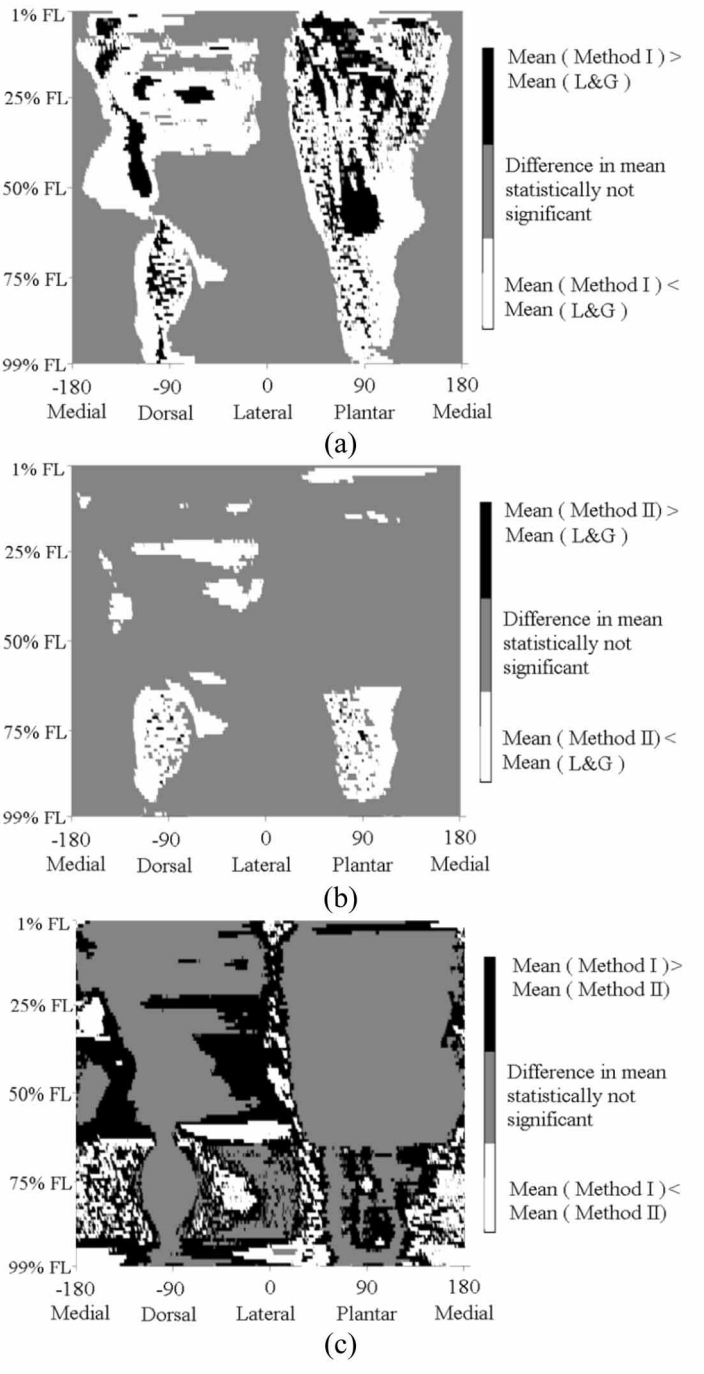

Figure 6. T-test ($n = 25$) to compare absolute error at each point (360 × 99) on the right foot using (a) Methods I and L&G, (b) Methods II and L&G, (c) Methods I and Method II (FL denotes foot length).

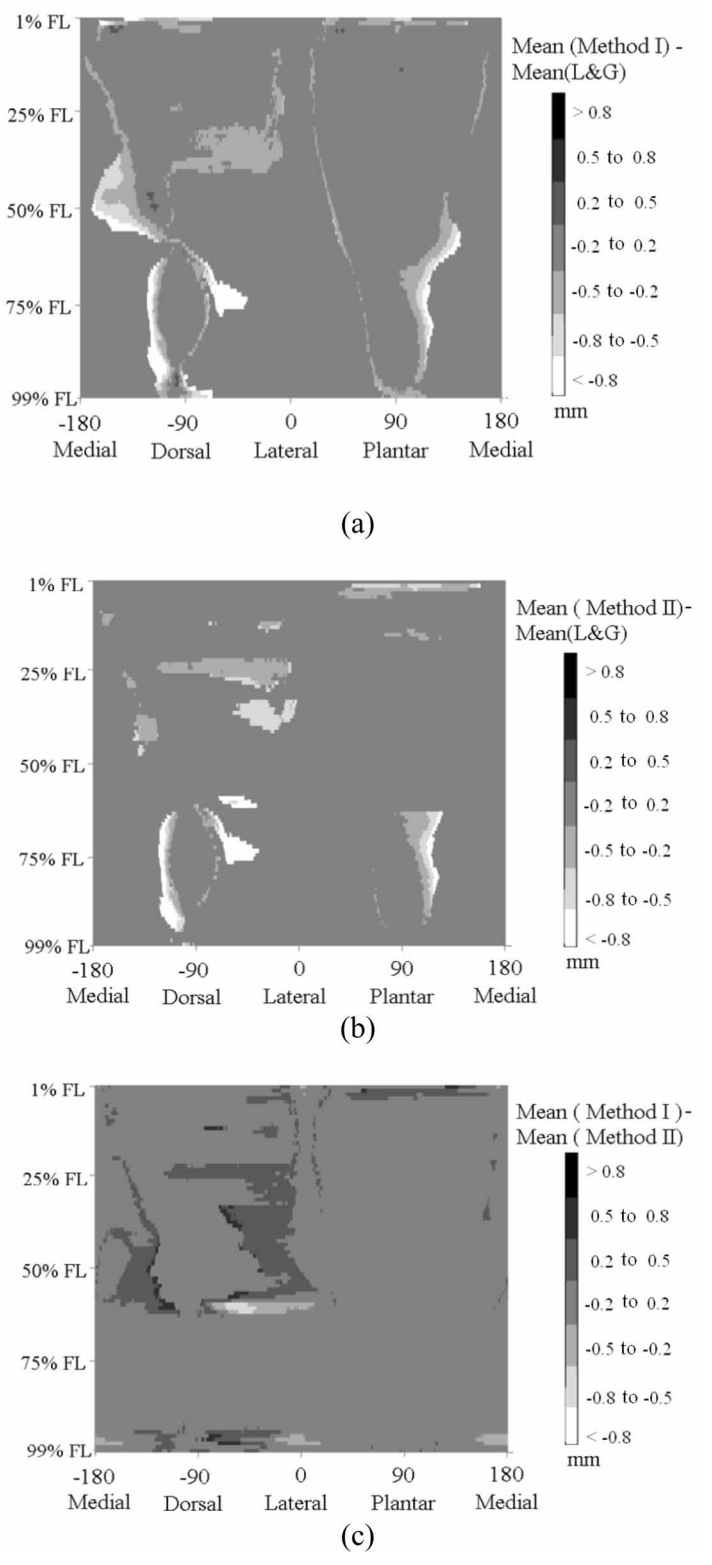

Figure 7. Comparison ($n = 25$) of absolute error at each point (360 × 99) on the right foot using (a) Methods I and L&G. (b) Methods II and L&G. (c) Methods I and II (FL denotes foot length).

medial talus, while it was relatively smaller (≈ -0.3) at the MPJ region and at the lateral side of fore foot (≈ -0.7). There were comparatively less errors at the plantar side of the toes. Most significant difference between methods I and II were on the dorsal side and at the plantar toe region. The difference in mean absolute error was generally greater (darker color) for method I compared to method II, except at the cuboid region where method II had larger absolute errors. Figure 8 shows sections at 10% of foot length intervals. This figure provides information on the relative position of each section relative to the 'actual' foot. Since anthropometric measures are still used for fitting shoes to feet, five anthropometric measures (ball width, ball girth, instep height, instep girth and heel width) were computed from the 3D data of the foot, predicted point cloud with L&G, predicted point cloud with Method I, and predicted point cloud with Method II). The instep height and girth were computed based on a transverse section at 50% of foot length, while the heel width was computed at 20% foot length from the pternion (back of heel). The mean, standard deviation, minimum and maximum values of the anthropometric measures are shown in table 4. There were no significant differences ($p < 0.05$) in the anthropometric measures among the four surfaces. However, the right foot was significantly larger than the left foot in ball width ($F(1,318) = 5.845$, $p = 0.016$) and the ball girth ($F(1,318) = 4.081$, $p = 0.044$).

4. Discussion

The objective of this paper was to predict the foot shape using two-dimensional outline views. Two methods were proposed. The first method used a foot outline and a foot height at 52% of foot length for right foot and 55% of foot length for left foot. Using this

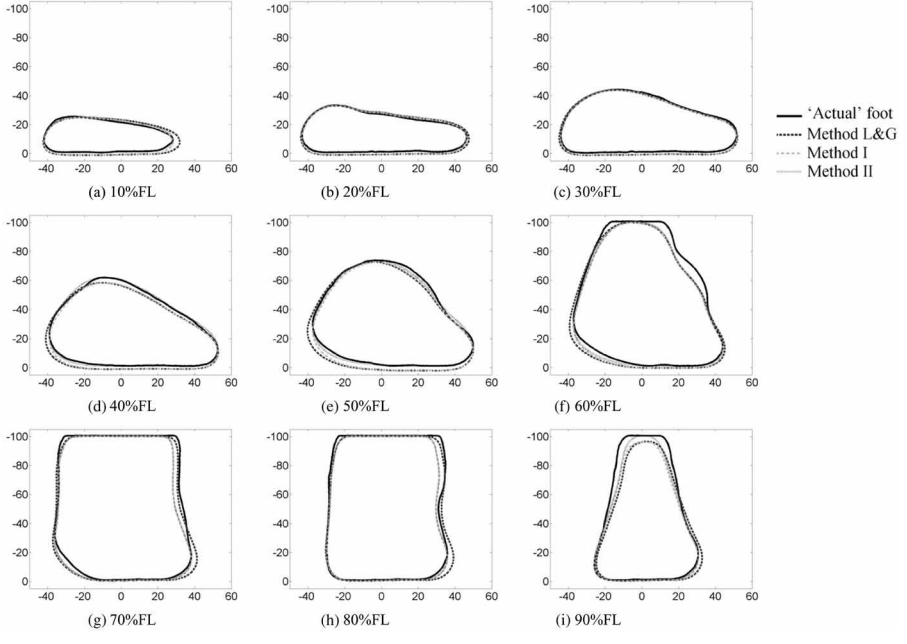

Figure 8. Sections of the foot of one subject compared with the output of different prediction methods. All units are mm.

Table 4. Mean, standard deviation, minimum and maximum anthropometric measures (mm) of the 'actual' feet and predicted feet using the three prediction methods (n = 40).

		Mean		SD.		Min.		Max.	
		Left	Right	Left	Right	Left	Right	Left	Right
Ball girth	'Actual'	237.9	239.7	10.7	10.1	214.1	217.3	264.8	268.9
	L&G	239.7	242.3	5.8	5.9	228.9	230.6	250.8	257.4
	Method I	237.6	239.9	10.5	10.1	216.9	219.7	264.1	269.3
	Method II	237.2	239.0	10.6	9.9	213.8	216.4	263.4	267.0
Ball width	'Actual'	97.7	98.8	4.8	4.5	88.5	90.0	109.6	111.3
	L&G	98.8	100.1	2.7	2.4	91.3	94.5	102.8	104.9
	Method I	97.7	98.8	4.8	4.5	88.5	90.0	109.6	111.3
	Method II	97.7	98.8	4.8	4.5	88.5	90.0	109.6	111.3
Instep girth	'Actual'	247.3	248.4	10.5	10.2	217.1	221.8	275.1	278.7
	L&G	250.5	251.6	7.5	7.6	236.0	237.1	270.0	269.8
	Method I	248.5	250.0	10.0	10.3	221.3	225.6	275.3	283.1
	Method II	246.8	247.8	10.3	10.1	218.9	223.0	277.2	279.0
Instep height	'Actual' feet	66.1	66.7	4.5	4.4	58.3	58.7	78.3	78.2
	L&G	67.3	68.1	4.0	4.4	60.2	60.9	77.1	78.4
	Method I	67.3	68.1	4.0	4.4	60.2	60.9	77.1	78.4
	Method II	66.1	66.7	4.5	4.4	58.3	58.8	78.3	78.2
Heel width	'Actual'	70.6	70.9	3.6	3.6	63.9	62.2	79.0	78.6
	L&G	71.2	72.0	2.8	2.9	64.0	66.0	76.0	77.6
	Method I	70.6	70.9	3.6	3.6	63.9	62.4	79.0	78.6
	Method II	70.6	70.9	3.6	3.6	63.9	62.4	79.0	78.6

method, a mean accuracy of 1.36 mm for the left foot and 1.37 mm for the right foot was obtained. The second method used foot outline and foot profile. This method produced a mean prediction accuracy of 1.02 mm for the left foot and 1.02 mm for the right foot. In general, method II seems to be more promising as it can capture the foot profile as well, thus increasing predictive accuracy. Even though an additional image is necessary for method II, obtaining the foot profile may be relatively easier than using an invasive method to obtain foot height for method I. While the cost of digital cameras, webcams and even mobile phone cameras are reducing, their resolution has been increasing. Hence the cost of these components will be relatively much lower than a digital laser scanner.

Once the required database of 'standard' feet are developed, individual foot shape can be predicted to relatively good accuracy using webcam, digital camera or even 35mm camera images. Even foot outlines drawn using paper and pencil together with height measures can be used to predict the foot shape to within 1.4 mm. Extensive statistical analysis performed using 35640 points on the surface of the foot has shown that errors are greater in the rear foot when using the Luximon and Goonetilleke (2004) model. Both the proposed methods have reduced the prediction error at the heel region. Method II has lower absolute errors in all regions except the cuboid region when compared to method I. Furthermore, there was more variation at the malleolus (talus) region possibly due to ankle joint movement when scanning. With the proposed model and existing transformations to convert foot shape to last shape (Adrian 1991), personalized lasts

may be manufactured. The proposed methods can be used to create the complete 3D foot shape without complex and expensive scanning of feet.

The predictive model validation was based on the 2D outline and foot profile obtained from the original 3D foot data. Even though images from webcams, digital cameras or even 35mm cameras can be used for this purpose, the error might be different due to image processing errors. Similar to the Luximon and Goonetilleke (2004) study, the prediction model can be further improved by using higher order polynomials to predict height, optimal number of sampling points, new scaling method and more control at the malleolus (or talus) region.

5. Conclusions

In this study, two methods were proposed to predict the foot shape. In the first method, the foot outline, foot height, and a standard foot shape was used while foot outline, foot profile (side-view), and a standard foot shape was used in the second to predict the 3D shape of a given foot. In the first method, the height at 52% of foot length for right foot and 55% of foot length for left foot were used to predict the height of all the other 98 cross sections of a foot using recursive regression equations. Similar to Luximon and Goonetilleke (2004), a standard foot shape was generated as the mean of forty Hong Kong male participants. The prediction models were validated using another set of 40 Hong Kong male subjects. The models were developed using 40 participants and then validated using another set of 40 participants. Mean accuracy of 1.36 mm for the left foot and 1.37 mm for the right foot was obtained using the first prediction method, while mean accuracy of 1.02 mm for the left foot and 1.02 mm for the right foot was obtained using the second prediction method. The method can be used to generate 3D foot shapes for custom footwear design.

Acknowledgements

The work described in this paper was supported by a grant from the Research Grants Council of the Hong Kong Special Administrative Region, China (Project No: HKUST 6162/02E) and the Hong Kong Polytechnic Research Office under the Postdoctoral Fellowship scheme.

References

Adrian, K. C. 1991, American last making: procedures, scale comparisons, sizing and grading information, basic shell layout, bottom equipment standards (Arlington, MA: Shoe Trades Publishing).

Bingham, A. W. and Rees, W. G. 1999, Construction of a high-resolution DEM of an Arctic ice cap using shape-from-shading, *International Journal of Remote Sensing*, **20,** 3231–3242.

Brannock 2004, http://www.brannock.com, December 1, 2004.

Choi, K. N., Worthington, P. L. and Hancock, E. R. 2002, Estimating facial pose using shape-from-shading, *Pattern Recognition Letters*, **23,** 533–548.

Gavrila, D. M. and Groen, F. C. A. 1992, 3D object recognition from 2D images using geometric hashing, *Pattern Recognition Letters*, **13,** 263–278

Goonetilleke, R. S, HO, C.-F. and SO, R. H.Y. 1997, Foot sizing beyond the 2-D Brannock method, IIE (HK). Annual Journal, 1997–1998, 28–31.

Hung, C. Y. P., Witana, C. P. and Goonetilleke, R. S. 2004, Anthropometric measurements from photographic images, *Proceedings of the 7th International conference on work with Computer Systems (WWCS),* 29 June–2 July 2004, Kuala Lumpur, Malaysia, 764–769.

Liu, H. 2003, Derivation of surface topography and terrain parameters from single satellite image using shape-from-shading technique, *Computers and Geosciences*, **29,** 1229 – 1239.

Luximon, A. and Goonetilleke, R. S. 2004, Foot Shape Modelling. *Human Factors* **46(2)**, 304 – 315.

Luximon, A., Goonetilleke, R. S. and Tsui, K. L. 2003, A 3-D Methodology to Quantify Footwear Fit, In M M Tseng and F Piller (eds), *The customer centric enterprise – advances in customization and personalization*. (New York/Berlin: Springer) 491 – 499.

Tam, K. S. and Atkinson, J. 2003, An approach for creating solid models from orthogonal views by identification of Boolean operations. *Journal of Materials Processing Technology*, **138,** 163 – 169.

Toutin, T. and Gray, L. 2000, State-of-the-art of elevation extraction from satellite SAR data, ISPRS, *Journal of Photogrammetry and Remote Sensing*, **55,** 13 – 33.

Triboulet, J., Z'Zi, E. C. and Chavand, F. 1996, Methods for updating the environment's geometric database in telerobotics, *Mathematics and Computers in Simulation*, **41,** 307 – 320.

Vorum Research Corporation 1998, On line help for Yeti shape builder version 3.0. Document Number 2700-8801-01. (Canada: Vorum Research Corporation).

Wildey, R. L. 1986, Radarclinometry for the Venus Radar Mapper. *Photogrammetric Engineering and Remote Sensing*, **52,** 41 – 50.